

Pep-1 Peptide-Modified Liposomal Carriers for Intracellular Delivery of Gold Nanoparticles

Myung Joo KANG,^a Sangyeop LEE,^b Bo Kyun KIM,^a Jae Yoon EUM,^a Sang Han PARK,^a
Min Hyung KANG,^a Chil Hwan OH,^c Jaebum CHOO,^{*,b} and Young Wook CHOI^{*,a}

^a College of Pharmacy, Chung-Ang University; Seoul 156–756, Republic of Korea; ^b Department of Bionano Engineering, Hanyang University; Ansan 426–791, Republic of Korea; and ^c College of Medicine, Korea University; Seoul 152–703, Republic of Korea. Received June 21, 2010; accepted October 14, 2010; published online November 1, 2010

A Pep-1 peptide-modified liposomal (Pep1-Lipo) carrier system was investigated to increase the intracellular delivery of gold nanoparticles (Au NPs). Au NPs with a mean diameter of 13 nm were successfully encapsulated into the inner aqueous compartment of the novel carrier using an ethanol injection technique, reserving the distinctive optical characteristics of the surface plasmon resonance peak around 530 nm. The Au NP-loaded liposomal carrier was physically characterized as 150–170 nm in size and 45 mV in zeta potential. Dark field microscopic observation demonstrated that *in vitro* cellular association and/or translocation of the nanoprobe into the cells was increased by Pep1-Lipo carriers compared to bare Au NPs. In conclusion, this novel liposomal formulation is a promising platform for the intracellular delivery of metallic nanoprobe including Au NPs.

Key words gold nanoparticle; liposome; Pep-1 peptide; nanocarrier; intracellular delivery

Recent advances in chemical engineering technology have guided the innovation of different metallic nanoparticles, including quantum dots, nanoshells, superparamagnetic nanoparticles, and gold nanoparticles (Au NPs).^{1–5} Au NPs are a promising tool for biomedical diagnosis because of their unique photo-optical properties, high sensitivity and biocompatibility. Their efficient scattering allows them to visualize and monitor subcellular compartments and cellular processes.^{4,6–8} In addition, Au NPs demonstrate therapeutic enhancement in radiation and photothermal therapies.^{9,10} However, diagnostic and therapeutic applications of Au NPs are significantly limited by several drawbacks, including aggregation of particles, loss of unique optical properties under physiological conditions, and poor translocation efficiency to the cytoplasm or nucleus.¹¹ The cellular uptake of nanoprobe with diameters between 12 nm and 70 nm was only about 4% for 24 h incubation.¹² Gold NPs as small as 10 nm are almost captured by membrane-bound organelles after cell incubation and do not reach the cytoplasm or nucleus.¹³

Liposomal nanocarrier systems are formidable tools for enhancing intracellular delivery of image probes, including Au NPs. Liposomes, composed of a lipid bilayer and internal aqueous compartment, are used as one of several sophisticated delivery technologies, since the entrapment of therapeutic and/or diagnostic agents in the carriers improves *in vivo* stability and promotes cellular uptake.^{14–16} We previously developed a Pep-1 peptide-modified liposomal (Pep1-Lipo) system, an advanced liposomal carrier designed to improve the intracellular delivery of macromolecules.¹⁷ The attachment of Pep-1 peptide (KETWWETW WTEWSQPKKKRKV), a cell-penetrating peptide, to carriers promoted the translocation of liposomal macromolecules into cells. Cell-penetrating peptides (CPPs), including Pep-1 peptide, rapidly cut across the plasma membrane for both high molecular weight drugs and particulate matter.^{18,19} We accordingly hypothesized that encapsulation of Au NPs into the Pep1-Lipo system facilitates the efficient transport of Au NPs to the cytoplasm.

In this report, an Au NP-loaded Pep1-Lipo carrier system was successfully prepared using an ethanol injection technique and characterized according to morphology, vesicular size, surface charge, loading efficiency, and optical spectrum patterns. Moreover, the *in vitro* cellular uptake proficiency of the novel carrier for Au NP delivery was determined.

Experimental

Chemicals and Reagents Soybean phosphatidylcholine (PC), Tween 80[®], cysteine, gold chloride trihydrate (HAuCl₄·3H₂O), and trisodium citrate (Na₃ citrate) were purchased from Sigma-Aldrich Co. (St. Louis, MO, U.S.A.). *N*-[4-(*p*-Maleimidophenyl)butyl]-phosphatidylethanolamine (MPB-PE) was obtained from Avanti Polar Lipids, Inc. (Alabaster, AL, U.S.A.). Pep-1 peptide (KETWWETW WTEWSQPKKKRKV, 22mer) was synthesized by Pepton Inc. (Daejeon, Korea). Cell culture materials were obtained from Invitrogen (Carlsbad, CA, U.S.A.). All other chemicals and reagents purchased from commercial sources were of analytical grade.

Preparation of Au NPs Au NPs were prepared using a process developed by Frens.²⁰ One hundred milliliters of 0.1% HAuCl₄ solution was heated to boiling point, and 10 ml of 1% Na₃ citrate solution was added immediately after boiling commenced. The mixture was boiled for 20 min and the pale yellow solution turned deep red, reflecting the formation of Au NPs.

Preparation of Au NP-Loaded Pep1-Lipo System The Au NP-entrapped Pep1-Lipo carrier was prepared by conjugating Pep-1 peptide to a nanoprobe-containing liposomal vesicle *via* a thiol-maleimide reaction as previously reported.¹⁷ Au NP-loaded vesicles were initially prepared using an ethanol injection method.^{21,22} Briefly, PC, Tween 80[®], and MPB-PE were taken in a molar ratio of 89:10:1.0 in ethanol at a lipid concentration of 20 mg/ml, then rapidly injected into a round bottom flask with Au NP solution (20 nm). After 30 min, the ethanol was evaporated under reduced pressure (Rotary Evaporator, Super fit; Ambala, India) to form Au NP-loaded vesicles. Unencapsulated Au NPs were removed by centrifugation at 15000 rpm for 20 min. Pep-1 peptide solution (1 mg/ml) was then added to the Au NP-loaded vesicles and allowed to react for 12 h at room temperature. Excess amounts of cysteine were added to block unreacted maleimide groups on the vesicles. Peptidyl liposomes were isolated from free Pep-1 peptide and cysteine using an ultrafiltration-stirred cell (Millipore, U.S.A.).

Characterization of Au NPs and Au NP-Loaded Pep1-Lipo Systems
Morphological Features: The appearance of Au NPs or Au NP-loaded Pep1-Lipo carriers was observed by transmission electron microscope (TEM) and cryogenic-temperature transmission electron microscope (Cryo-TEM), respectively. A small drop of Au NP dispersion was placed on a collodion-coated grid and drawn off with filter paper. Phosphotungstic acid (2%, w/v) was applied to the grid and the stained sample was air-dried. The grid was examined under an electron microscope (JEOL-model JEM-2000EXII, Japan). The liposomal suspension was placed onto holey-carbon film-sup-

* To whom correspondence should be addressed. e-mail: ywchoi@cau.ac.kr; jbchoo@hanyang.ac.kr

ported grids for observation of the Au NP-loaded Pep1-Lipo. A thin aqueous film was produced by blotting with filter paper. The grids were immediately plunged into liquid ethane before the thin samples began to evaporate. The frozen grids were stored in liquid nitrogen and transferred to a Gatan model-630 cryotransfer (Gatan, Inc., Warrendale, PA, U.S.A.) under liquid nitrogen at -190°C . Cryo-TEM images were then acquired with a CCD camera (Multiscan 600W, Gatan, Inc.).

Size and Zeta Potential: Nanoparticles or liposomal vesicles were diluted with an appropriate volume of water and examined for size distribution and zeta potential using a dynamic light scattering (DLS) particle size analyzer (Zetasizer Nano-ZS, Malvern Instrument; Worcestershire, U.K.) equipped with a 50 mV laser at a scattering angle of 90° . All measurements were carried out under ambient conditions in triplicate.

Loading Amount: Isolated Au NP-loaded peptidyl liposomes (0.5 ml) were disrupted with 5 ml of 10% Triton X-100 to obtain a clear solution. The amount of Au NPs in the obtained solution was determined using UV-Vis spectrometer at 528 nm. The loading amount per total lipid was calculated by $C/W \times 100$, where C is the amount of Au NPs encapsulated in the liposomes and W is the amount of lipid used in the formulation.²²⁾

UV-Vis Absorbance Spectroscopy: UV-Vis absorption spectrums of Au NPs and Au NP-loaded liposomal suspensions were measured in the range of 400 to 600 nm using a UV-Vis spectrophotometer (Shimadzu UV-160, Japan) at 25°C with a 1 cm quartz cuvette.

In Vitro Cellular Uptake Behavior Human breast adenocarcinoma (MCF-7) and squamous carcinoma cells (SCC) were cultured in Dulbecco's modified Eagle's medium (DMEM) supplemented with 10% fetal bovine serum. Cells were incubated at 37°C in a water saturated incubator with 5% CO_2 . For cellular uptake studies, cells were seeded in a growth medium at a density of 1.0×10^5 per well on a 6-well plate with a cover slip. Au NPs and Au NP-loaded Pep1-Lipo (2.5 mg/ml) were added to cells and incubated for 1 h at 37°C . Cells were then washed three times with phosphate buffered saline (PBS) solution and fixed in 3.7% formaldehyde. Cells were mounted and Au NP scattered light was visualized using the Olympus IX-71 microscope assembled with a home-made dark-field condenser.

Results and Discussion

Characteristics of Au NPs Au NP dispersion resulting from Au ion reduction with citric acid was evaluated according to morphology, particle size, zeta potential, and UV-Vis absorption spectrum. TEM micrographs demonstrated that the Au NPs were spherical or ellipsoidal with homogeneous particle sizes in the range of 10 to 15 nm (Fig. 1a). However,

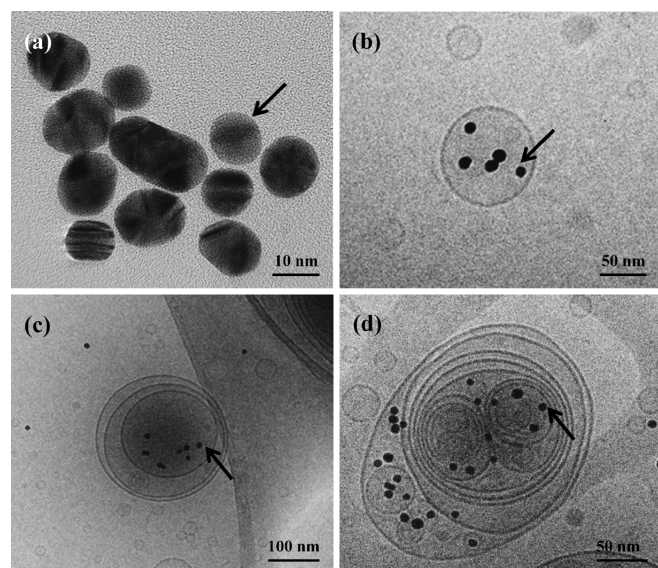


Fig. 1. Cryo-TEM Images of Au NPs (a) and Au NP-Loaded Pep1-Lipo Nanocarriers (b–d)

Micrographs demonstrate several types of Au NP-loaded vesicular systems, including small unilamellar vesicles (SUVs) (b), multilamellar vesicles (MLVs) (c), and multivesicular liposomes (MVLs) (d). Arrows indicate Au NP.

the hydrodynamic diameter of the nanoprobe was determined to be approximately 28 nm using a DLS analyzer (Table 1), which is a greater value than previously determined under microscopic observation. The DLS system is sensitive to the double layer surrounding Au NPs in the aqueous dispersion, which in turn, leads to a misrepresentation of particle diameter, making the NPs appear larger than they actually are.²³⁾ The surface charge of Au NPs was approximately -60 mV due to an anionic stabilizer, which contributes to hydrophilicity at the surface of the nanoparticle and facilitates repulsive forces between particles to form stable nanodispersion. Gold NPs exhibited a strong surface plasmon resonance (SPR) band around 530 nm (Fig. 2), which arose from the coherent electron oscillation of surface gold atoms induced by the incident electromagnetic field.²⁴⁾ Strong absorption in the visible SPR band region is a unique property of Au NPs, making them promising for use as colorimetric nanoprobe. Citrate-stabilized small Au NPs, which are commonly used in medical applications, were successfully fabricated and used in a further investigation of liposomal encapsulation to facilitate efficient cellular translocation.

Characteristics of Au NP-Loaded Pep1-Lipo Systems

There are three types of Au NP-liposomal complexes.^{14,15,25,26)} The first is a liposome containing Au NPs in the inner aqueous phase, the second contains Au NPs in the lipid membrane, and the third is a liposome modified with Au NPs on the surface. The Au NP-loaded carrier system used in our study is the first type, because entrapment of Au

Table 1. Physical Characteristics of Au NPs and Au NP-Loaded Pep1-Lipo Carriers

	Au NPs	Au NP-loaded Pep1-Lipo
Size (nm)		
$d_{\text{TEM}}^{\text{a)}$	13.3 ± 2.2	152.9 ± 35.3
$d_{\text{DLS}}^{\text{b)}$	28.4 ± 4.7	170.9 ± 18.7
Polydispersity index	0.242 ± 0.072	0.176 ± 0.025
Zeta potential (mV)	-60.2 ± 5.6	44.8 ± 3.6
Loading amount (pmol/mg) ^{c)}	—	0.071 ± 0.008

a) Diameters of Au NPs and Pep1-Lipo carriers determined by TEM and cryo-TEM observation, respectively. b) Diameters determined using a DLS particle size analyzer. c) pmol/mg indicates the amount of Au NP loaded per total lipid used. Values represent mean \pm S.D. ($n=3$).

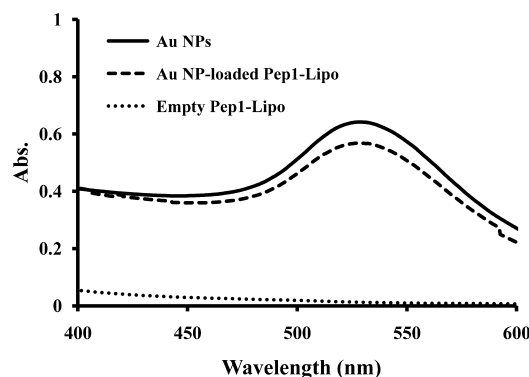


Fig. 2. UV-Vis Absorption Spectra of Au NPs and Au NP-Loaded Pep1-Lipo Carriers

A strong SPR band around 530 nm indicates that Au NPs retain their unique optical properties in the liposomal carrier.

NPs in the inner compartment provides the benefit of shielding nanoprobe from environmental circumstances. Cryo-TEM observation clearly demonstrated that several liposomal structures, including small unilamellar vesicles (SUVs) (Fig. 1b), multilamellar vesicles (MLVs) (Fig. 1c), and multivesicular liposomes (MVLs) (Fig. 1d), were formed using an ethanol injection method in the 50 to 200 nm range. Gold NPs as small as about 13 nm were located in the inner aqueous compartment, regardless of vesicular type. Following ethanol evaporation, phospholipids spontaneously adopted a bilayer organization in the aqueous solution to form closed vesicular structures. Meanwhile, Au NPs, which were dispersed in the aqueous solution, were encapsulated in the inner section of the carrier. The thickness of the liposomal bilayer, which was previously reported to be approximately 4 nm,²⁷⁾ and the relatively large diameter of the Au NPs (11 nm) further partitioned the nanoprobe into the inner compartment of the carriers. In a previous report, hydrophobic Au NPs with a mean diameter of 1.5 nm, which is thinner than the lipid bilayer, were embedded primarily within vesicular membranes, while larger Au NPs (5 nm) were centered primarily inside the vesicles.²⁸⁾ Although the number of Au NPs entrapped in the vesicle varied from 1–40 per vesicle, approximately five particles were counted per vesicle with no aggregation.

Consistent with cryo-TEM observation of 150 nm, the average diameter of Pep1-Lipo measured by DLS spectrometer was 170 nm (Table 1), a value that is effective for intracellular delivery. Garbuzenko *et al.* also demonstrated that 150 nm stealth liposomes consisting of PC, cholesterol, and polyethylene glycol-grafted phosphatidylethanolamine resulted in the highest levels of cell uptake and accumulation in solid tumors, compared to vesicles that were 100, 350, or 450 nm in size.²⁹⁾ Pep1-Lipo carriers demonstrated a positive charge of 45 mV due to the conjugation of cationic peptides to vesicular surfaces. We previously determined that 730 molecules of Pep-1 peptides are attached to each vesicle.¹⁷⁾ Obtaining the absorbance spectra is important for determining Au NP stability, since Au NP aggregation induces the loss of their unique SPR peak. As shown in Fig. 2, the distinctive SPR peak of Au NP at 528 nm was observed in Au NP-loaded carriers, indicating that Au NPs were stably dispersed in the aqueous compartment of the vesicle without aggregation or degradation during and/or after the encapsulation process. These results are consistent with cryo-TEM observations.

In Vitro Cellular Uptake Behavior Cellular uptake of the Au NP-loaded Pep1-Lipo carrier was investigated in live cells using a dark field microscopy. As shown in Figs. 3a and c, bare Au NPs exhibited minimal intracellular accumulation over 1 h, as indicated by much weaker photointensity in MCF-7 and SCC cells. Gold NPs primarily resided at the cellular membrane and were unable to reach the cytoplasm or nucleus. In contrast, cellular association and/or internalization of the nanoprobe drastically increased by means of Pep1-Lipo carriers in both cell lines, which presented stronger photointensity throughout the cytoplasm (Figs. 3b, d). The liposomal vesicle carries the nanoprobe while the Pep-1 peptide attached to the surface of the carrier efficiently promotes the transfer of liposomal nanoprobe into the cells. Structurally, the hydrophobic tryptophan-rich domain of the Pep-1 peptide binds Pep1-Lipo to the cellular

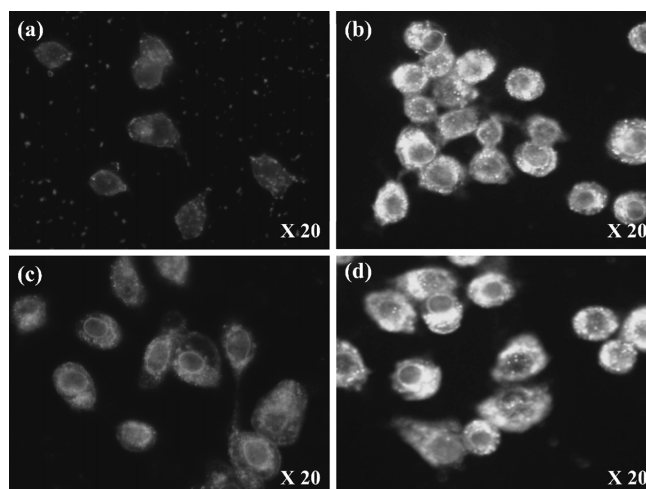


Fig. 3. Dark Field Light Scattering Images of MCF-7 Cells Treated with Au NPs (a), Au NP-Loaded Pep1-Lipo (b), SCC Cells Incubated with Au NPs (c), and Pep1-Lipo (d) at 37 °C and pH 7.4 for 1 h

In contrast to the minimal intracellular accumulation of the nanoprobe alone, the Pep1-Lipo system drastically increases the cellular association and internalization of Au NPs in both MCF-7 and SCC cells.

membrane and the cationic lysine-rich domain subsequently triggers the internalization of liposomal nanoprobe.^{30,31)} Our earlier study demonstrated that Pep-1 peptide-modified liposomes significantly increased cellular association in proportion to the number of peptides on the liposomal surface, revealing better cellular internalization of entrapped macromolecules compared to that of conventional liposomes.¹⁷⁾ Similarly, Antennapedia (one of the CPPs)-coupled liposomes showed higher uptake behavior into a panel of cell lines than unmodified liposomes, representing the enhanced intracellular delivery of a large variety of liposome-entrapped molecules.³²⁾ From these findings, we assure that linkage of Pep-1 peptide to the liposomal surface would lead to enhanced translocation of liposomal Au NPs into the cells, compared to either conventional liposomes free from peptide modification or bare Au NPs.

Several strategies have been reported for the intracellular delivery of metallic nanoparticles, including microinjection,³³⁾ cationic transfection reagents,³⁴⁾ CPPs introduction,^{35,36)} and electroporation.³⁷⁾ Although these techniques facilitate better transport of Au NPs to the cells, they present certain problems such as a limited throughput process in microinjection requiring simultaneous manipulation of individual cells and invasive damage to cellular membranes in electroporation. When CPPs form noncovalent complexes with nanoprobe, the dissociation of penetrating peptides in the blood decreases translocation capacity *in vivo*.³⁸⁾ Alternatively, incorporating Au NPs into the Pep1-Lipo carrier system not only enhances intracellular delivery but also improves physical and/or biological stability with prolonged circulation time *in vivo*. In considerations of clinical application, this nanoprobe-loaded liposomal system could be principally beneficial as a tool to visualize subcellular compartments and microenvironment. In addition, depending on the properties of entrapped metallic NPs, the system can be applicable as a promising platform to monitor the cellular procedures, such as probing intracellular pH, detecting intracellular constituents, and even elucidating the biochemical in-

teraction with its translocation capability.³⁹⁾ Future studies should focus on optimizing this platform by testing *in vivo* biodistribution, and controlling the physical and optical characteristics of liposomal carrier or metallic NPs.

Conclusion

This study illustrates that our novel Pep-1 peptide-modified carrier system is effective for the enhanced intracellular delivery of Au NPs. The Pep1-Lipo carriers efficiently encapsulate citrate-stabilized nanoprobe in the inner aqueous compartment, while maintaining the distinctive optical characteristics of the nanoprobe. Due to their translocation capabilities, these novel liposomal carriers will be further evaluated for *in vivo* biodistribution as well as clinical applications.

Acknowledgments This work was supported by the Chung-Ang University Research Grants in 2010.

References

- Colvin V. L., Schlamp M. C., Alivisatos P., *Nature* (London), **370**, 354–357 (1994).
- Alivisatos P., *Nature Biotechnol.*, **22**, 47–51 (2003).
- Souza G. R., Christianson D. R., Staquicini F. I., Ozawa M. G., Snyder E. Y., Sidman R. L., Miller J. H., Arap W., Pasqualini R., *Proc. Natl. Acad. Sci. U.S.A.*, **103**, 1215–1220 (2006).
- Kneipp J. K., Kneipp H., McLaughlin M., Brown D., Kneipp K., *Nano Lett.*, **6**, 2225–2231 (2006).
- Jin H., Heller D. A., Strano M. S., *Nano Lett.*, **8**, 1577–1585 (2008).
- Chourpa I., Morjani H., Riou J. F., Manfait M., *FEBS Lett.*, **397**, 61–64 (1996).
- Kneipp K., Haka A. S., Kneipp H., Badizadegan K., Yoshizawa N., Boone C., Shafer-Peltier K. E., Motz J. T., Dasari R. R., Feld M. S., *Appl. Spectrosc.*, **56**, 150–154 (2002).
- Talley C. E., Jusinski L., Hollars C. W., Lane S. M., Huser T., *Anal. Chem.*, **76**, 7064–7068 (2004).
- Hainfeld J. F., Slatkin D. N., Smilowitz H. M., *Phys. Med. Biol.*, **49**, 309–315 (2004).
- Pissuwan D., Valenzuela S. M., Cortie M. B., *Trends Biotechnol.*, **24**, 62–67 (2006).
- Shamsaie A., Jonczyk M., Sturgis J., Paul Robinson J., Irudayaraj J., *J. Biomed. Opt.*, **12**, 020502 (2007).
- Ponti J., Colognato R., Franchini F., Gioria S., Simonelli F., Abbas K., Uboldi C., Kirkpatrick C. J., Holzwarth U., Rossi F., Nanotoxicology-2nd International Conference, Zürich, 7–10 September, 2008.
- Chithrani B. D., Ghazani A. A., Chan W. C. W., *Nano Lett.*, **6**, 662–668 (2006).
- Kojima C., Hirano Y., Yuba E., Harada A., Kono K., *Colloids Surf. B Biointerfaces*, **66**, 246–252 (2008).
- Pal A., Shah S., Kulkarni V., Murthy R. S. R., Devi S., *Mater. Chem. Phys.*, **113**, 276–282 (2009).
- Chithrani D. B., Dunne M., Stewart J., Allen C., Jaffray D. A., *Nanomedicine*, **6**, 161–169 (2010).
- Kang M. J., Kim B. G., Eum J. Y., Park S. H., Choi S. E., An J. J., Jang S. H., Eum W. S., Lee J., Lee M. W., Kang K., Oh C. H., Choi S. Y., Choi Y. W., *J. Drug Target.*, Published online, 25 August 2010. doi : 10.3109/1061186X.2010.511226
- Schwarze S. R., Dowdy S. F., *Trends Pharmacol. Sci.*, **21**, 45–48 (2000).
- Josephson L., Tung C. H., Moore A., Weissleder R., *Bioconjug. Chem.*, **10**, 186–191 (1999).
- Frens G., *Nat. Phys. Sci.*, **241**, 20–22 (1973).
- Sachse A., Leike J. U., Rössling G. L., Wagner S. E., Krause W., *Invest. Radiol.*, **28**, 838–844 (1993).
- Fan M., Xu S., Xia S., Zhang X., *Eur. Food Res. Technol.*, **227**, 167–174 (2008).
- Diegoli S., Manciuola A. L., Begum S., Jones I. P., Lead J. R., Preece J. A., *Sci. Total Environ.*, **402**, 51–61 (2008).
- Mie G., *Ann. Phys.*, **25**, 377–445 (1908).
- Li X., Li Y., Yang C., Li Y., *Langmuir*, **20**, 3734–3739 (2004).
- Paasonen L., Laaksonen T., Johans C., Yliperttula M., Kontturi K., Urtti A., *J. Controlled Release*, **122**, 86–93 (2007).
- Park S. H., Oh S. G., Mun J. Y., Han S. S., *Colloids Surf. B Biointerfaces*, **48**, 112–118 (2006).
- Holmberg A. L., *NNIN REU Research Accomplishments*, **2008**, 14–15 (2008).
- Garbuzenko O., Saad M., Ber E., Zhang M., Vetcher A., Soldatenkov V., Minko T., AAPS 2007 Annual Meeting. [Online] Available at: www.aapsj.org/abstracts/AM_2007/AAPS2007-002942.PDF
- Deshayes S., Heitz A., Morris M. C., Charnet P., Divita G., Heitz F., *Biochem.*, **43**, 1449–1457 (2004).
- Henriques S. T., Castanho M. A., *J. Pept. Sci.*, **14**, 482–487 (2008).
- Marty C., Meylan C., Schott H., Ballmer-Hofer K., Schwendener R. A., *Cell Mol. Life Sci.*, **61**, 1785–1794 (2004).
- McDougall C., Stevenson D. J., Brown C. T. A., Gunn-Moore F., Dhoklakia K., *J. Biophotonics*, **2**, 736–743 (2009).
- Voura E. B., Jaiswal J. K., Mattoussi H., Simon S. M., *Nat. Med.*, **10**, 993–998 (2004).
- Rozenzhak S. M., Kadakia M. P., Caserta T. M., Westbrook T. R., Stone M. O., Naik R. R., *Chem. Commun.*, **17**, 2217–2219 (2005).
- Mandal D., Maran A., Yaszemski M. J., Bolander M. E., Sarkar G., *J. Mater. Sci. Mater. Med.*, **20**, 347–350 (2009).
- Chen F. Q., Gerion D., *Nano Lett.*, **4**, 1827–1832 (2004).
- Ignatovich I. A., Dizhe E. B., Pavlotskaya A. V., Akifiev B. N., Burov S. V., Orlov S. V., Perevozchikov A. P., *J. Biol. Chem.*, **278**, 42625–42636 (2003).
- Shamsaie A., Jonczyk M., Sturgis J., Robinson J. P., Irudayaraj J., *J. Biomed. Opt.*, **12**, 020502 (2007).